Theoretical and Applied Climatology
https://doi.org/10.1007/s00704-023-04660-5

RESEARCH

Highlighting climate change by applying statistical tests and climate indices to the temperature of Kébir Rhumel watershed, Algeria

Abdesselem Kabour[1] · Lynda Chebbah[2]

Received: 15 July 2023 / Accepted: 15 September 2023

Abstract
A number of statistical methods (Mann-Kendall, Pettitt test, etc.) and climatic indices (Emberger, Euverte) were used to highlight climate change in the Kébir Rhumel watershed, at seven geographically selected stations, by studying temperature on a monthly scale. The time series used was from 1901 to 2021 (121 years). The results show a breakpoint in the series, identified at 1980, for all the stations. Analysis of the monthly temperature values, before and after the breakpoint, shows an increase of between 1.08 and 1.18 °C. The graphical representation of the climatic indices indicates that most of the stations moved from the sub-humid stage (before the break) to the semi-arid stage (after the break). Euverte's method displays that the temperatures for 80% of the months are shifting towards a warmer, less humid climate.

1 Introduction

Climate is a key component of the Earth system and is made up of several variables (temperature, rainfall). Analyzing their long-term variations is important for studying climate change, especially temperature (Panda and Sahu 2019). The impact of climate change on its constituent elements, such as temperature and precipitation, is an indisputable fact, studied and proven by several authors (Dai 2011; Ahmed et al. 2018; Di Cecco and Gouhier 2018; Sam et al. 2019). The problem has been approached using a number of statistical methods (Wu et al. 2012; Rauf et al. 2016) or by spatial distribution (Wu et al. 2012) or simulative and predictive (Lubes-Niel et al. 1998). Studies have also focused on the temperature variation impact on water resources at watershed level (Wang et al. 2014) on hydrological regimes (Moral 1964; Güçlü 2018) on crops (Gilman et al. 2010) on its drought-aggravating effect (Dai 2011; Wang et al. 2017; Ahmed et al. 2018; Sam et al. 2019; Derdous et al. 2021).

African temperature statistical analysis series between 1979 and 2010 reveals significant upward trends across Africa (Collins 2011). It also examines temperature changes over time, detecting abrupt changes in the data series and revealing statistically significant changes in the analysed variable, such as increasing temperature values (Akinsanola and Ogunjobi 2014) (Akinsanola and Ogunjobi 2014).

Several climate indices have been developed by scientists and are available in the scientific literature. They are used for different analyses of climate data, depending on the availability of data and the objective of the study. These applications and their interpretations provide a comprehensive summary of temperature variability and these indices have been calculated and mapped at different time scales (monthly, seasonal and annual). These applications have made it possible to highlight climate variability and study its dynamics in a highly informative spatiotemporal framework (Neira Mendez 2005; Asfaw et al. 2018) (Neira Mendez 2005; Asfaw et al. 2018).

A precise climatic classification based on the aridity index, using temperature values as the determining variable. This assessment, together with the spatial distribution of these indices in the region, is an effective tool for decision support in the management of agriculture, water resources and urban planning (Derdous et al. 2021).

The availability of climate data (long time series) and the large number and good spatial distribution of climate stations in the region under study make it possible to maximize the information and simplify the choice of methods used. This option also makes it possible to detect seasonal

✉ Abdesselem Kabour
kabour_abs@yahoo.fr

Lynda Chebbah
cheblyn@yahoo.fr

[1] University Centre of Mila, Mila, Algeria

[2] Modelling and Socio-Economic Analysis in Water Sciences Laboratory, MASESE Lab, University of Souk Ahras, Souk Ahras, Algeria

Published online: 22 September 2023

and annual anomalies for the different variables at the level of each station analyzed, as a function of time, in order to study trends and predictions (Singh et al. 2008).

The aim of this work is to demonstrate the application of statistical methods to the analysis of climate data series and their ability to detect anomalies using statistical tests chosen according to the purpose sought. These anomalies are interpreted as an indication of climate change, i.e., an increase in temperature, after a break in the series analyzed, which is then quantified as a percentage.

2 Materials and methods

2.1 Area of study

The Kébir-Rhumel watershed (WS), with a surface area of 8831 km^2 and a perimeter of 1151 km, is located in northeast Algeria (Fig. 1). It is bounded to the north by the Côtiers Constantinois Centre and West watershed (WS03), to the south by the Hauts Plateaux Constantinois watershed (WS07), to the west by the Soummam watershed (WS15), and to the east by the Seybouse watershed (WS14). It has a

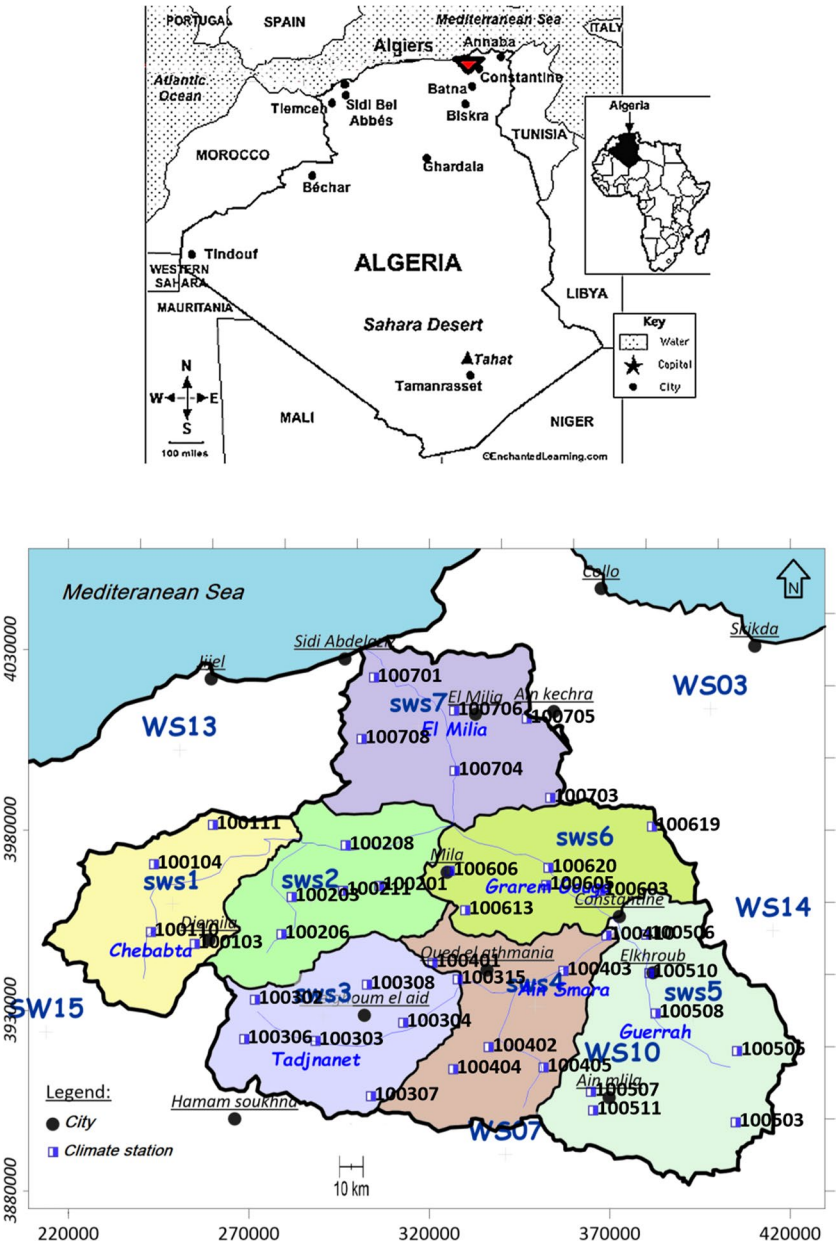

Fig. 1 Geographical location of the Kébir Rhumel watershed (WS 10) and location of the sub-watershed (Sws) and climatic stations

Table 1 Characteristics of selected climate stations in WS 10, series 1901–2021 (Pavg, annual rainfall sums average; Tavg, annual temperatures average; SD, standard deviation)

1902/2021	Code	Stations selected	Tmin (°C)	Tmax (°C)	SD (T)	T avg (°C)	P avg (mm)
sws1	100110	Chebabta	13.53	16.24	0.68	14.69	495.75
sws2	100211	Tiberguent	13.89	16.65	0.69	15.02	508.88
sws3	100303	Tadjnanet	13.52	14.23	0.67	15.38	496.44
sws4	100403	Ain Smara	13.50	16.26	0.71	14.62	572.39
sws5	100508	Guerrah	13.51	16.25	0.71	13.93	573.09
sws6	100620	Grarem Gouga	15.04	17.71	0.69	16.18	651.29
sws7	100706	El Milia	15.03	17.72	0.68	15.49	652.00

coastline of around 07 km and is spread geographically over six districts: Oum El Bouaghi, Skikda, Constantine, Mila, Sétif, and Jijel (Oulhaci 2016; Aidat 2017).

The Kébir Rhumel consists of seven sub-watershed (sws): these are Kebir Wadi (sws1), Endja Wadi (sws2), Rhumel Wadi upstream (sws3), Rhumel Wadi downstream (sws4), Boumezroug Wadi (sws5), Smendou Wadi (sws6), and finally, Kébir Rhumel Wadi (sws7) (Fig. 1); they form a highly branched and dense stream networks totalling around 8.000 km in length. Two dams are in operation in this basin: Beni Haroun and Hammam Grouz (Abdeddaim 2018).

The Kébir Rhumel catchment is equipped with an observation network of 42 climate stations (all recording temperature and precipitation) (Fig. 1) (Oulhaci 2016; Aidat 2017). To carry out this work, seven climate stations (Fig. 1) were selected for their representative geographical location, spread over the seven sub-catchments (Fig. 1). They are presented with their characteristics in Table 1, namely Chebabta, Tiberguent, Tadjnanet, Ain Smara, Guerrah, Grarem Gouga and El Milia.

2.2 Data description

The data used in this work are those measured by the National Water Resources Agency, supplemented by those from the "https://power.larc.nasa.gov/data-access-viewer/" website.

The data collected are temperature values from 1901 to 2021, from which monthly and annual averages have been derived. For the selected stations, the average annual maximum temperatures range from 14.23 °C in Tadjenant to 17.72 °C in El Milia, and the average minimum temperatures are from 13.50 °C in Ain Smara to 15.04 °C in Grarem Gouga (Table 1). For the same series of years 1901–2021, the average annual temperature in the Kebir Rhumel varies from 13.93 °C at the Guerrah station to 16.18 °C at the Grarem Gouga station (Table 1).

Table 2 Summary table of the different tests applied to the seven selected stations

Series: 1902/2021		Chebabta	Tiberguent	Tadjnanet	Ain Smara	Guerrah	Grarem Gouga	El Milia
Sub-watershed		sws1	sws2	sws3	sws4	sws5	sws6	sws7
Station code		100110	100211	100303	100403	100508	100620	100706
Mann Kendall test	Kendall rate $Z<1.96$	0.566	0.571	0.566	0.580	0.580	0.565	0.565
	$S>0$ (Increase)	4107	4142	4107	4205	4205	4099	4099
	Var (S)	166,858.33	202,660.94	166,858.33	244,148.63	244,148.63	192,957.39	192,957.39
	p value (bilateral)	<0.0001	<0.0001	<0.0001	<0.0001	<0.0001	<0.0001	<0.0001
	Alpha: α	0.05	0.05	0.05	0.05	0.05	0.05	0.05
Slope of Sen (°C)		0.0150	0.0158	0.0152	0.0164	0.0164	0.0156	0.0156
Buishand test (Q)		42,810	43,913	42,809	44,146	44,146	43,686	43,686
Null hypothesis ($p<\alpha$)		Rejected	Rejected	Rejected	Rejected	Rejected	Rejected	Rejected
Hubert segmentation	Break Year (BP)	1980	1980	1980	1980	1980	1980	1980
	Scheffé test	1%	1%	1%	1%	1%	1%	1%
	Year start–end	1901–1980	1901–1980	1901–1980	1901–1980	1901–1980	1901–1980	1901–1980
		1981–2021	1981–2021	1981–2021	1981–2021	1981–2021	1981–2021	1981–2021
	Moy before BP	14.33	14.64	14.33	14.24	14.23	15.8	15.81
	Moy after BP	15.39	15.76	15.39	15.39	15.38	16.91	16.91
Rate of increase	(%)	7.40	7.65	7.40	8.09	8.08	7.03	6.96
	(°C)	1.09	1.15	1.14	1.18	1.13	1.14	1.08

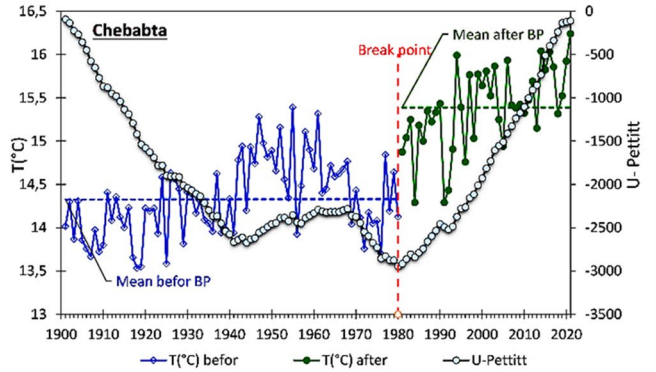
Chebabta
Break point
Mean after BP
Mean befor BP
T(°C)
U- Pettitt
T(°C) befor
T(°C) after
U-Pettitt

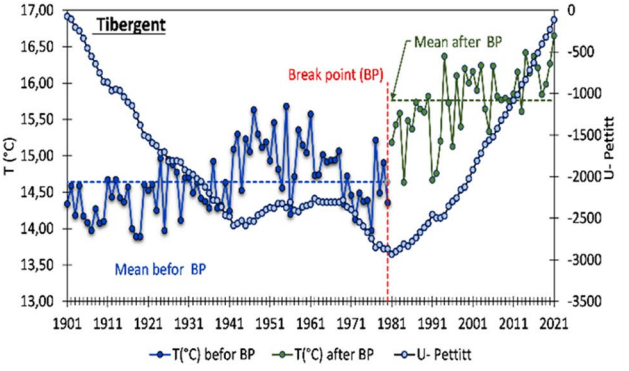
Tibergent
Break point (BP)
Mean after BP
Mean befor BP
T (°C)
U- Pettitt
T(°C) befor BP
T(°C) after BP
U- Pettitt

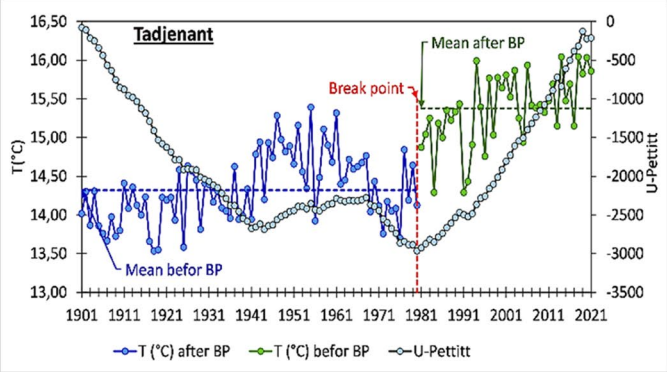
Tadjenant
Break point
Mean after BP
Mean befor BP
T (°C)
U-Pettitt
T (°C) after BP
T (°C) befor BP
U-Pettitt

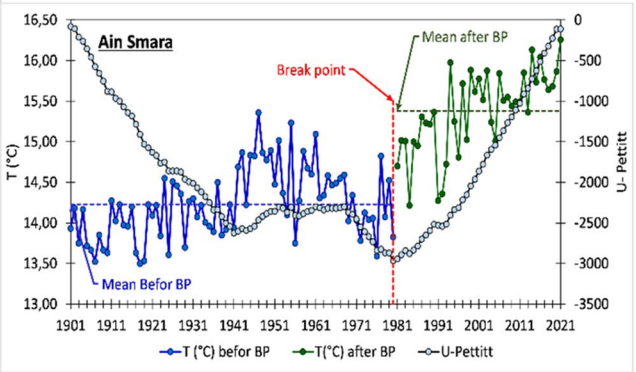
Ain Smara
Break point
Mean after BP
Mean Befor BP
T (°C)
U- Pettitt
T (°C) befor BP
T(°C) after BP
U-Pettitt

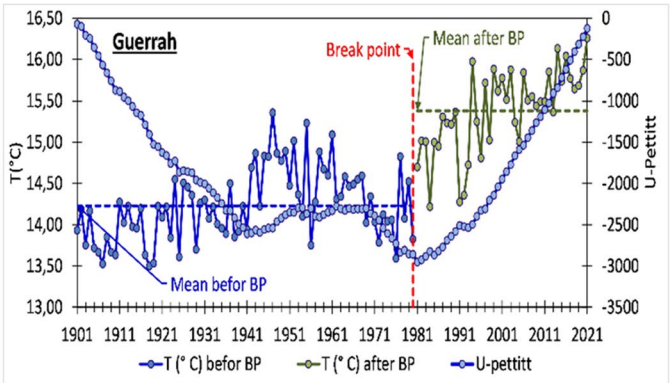
Guerrah
Break point
Mean after BP
Mean befor BP
T (°C)
U-Pettitt
T (° C) befor BP
T (° C) after BP
U-pettitt

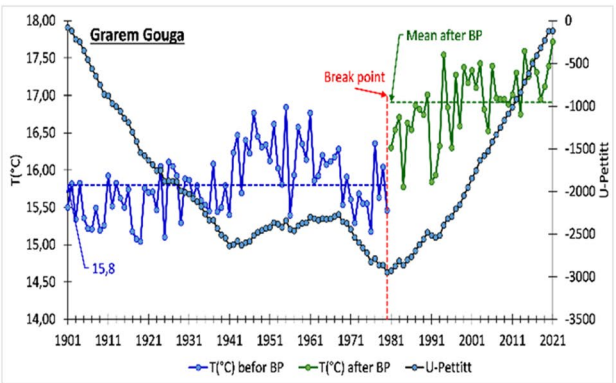
Grarem Gouga
Break point
Mean after BP
15,8
T(°C)
U-Pettitt
T(°C) befor BP
T(°C) after BP
U-Pettitt

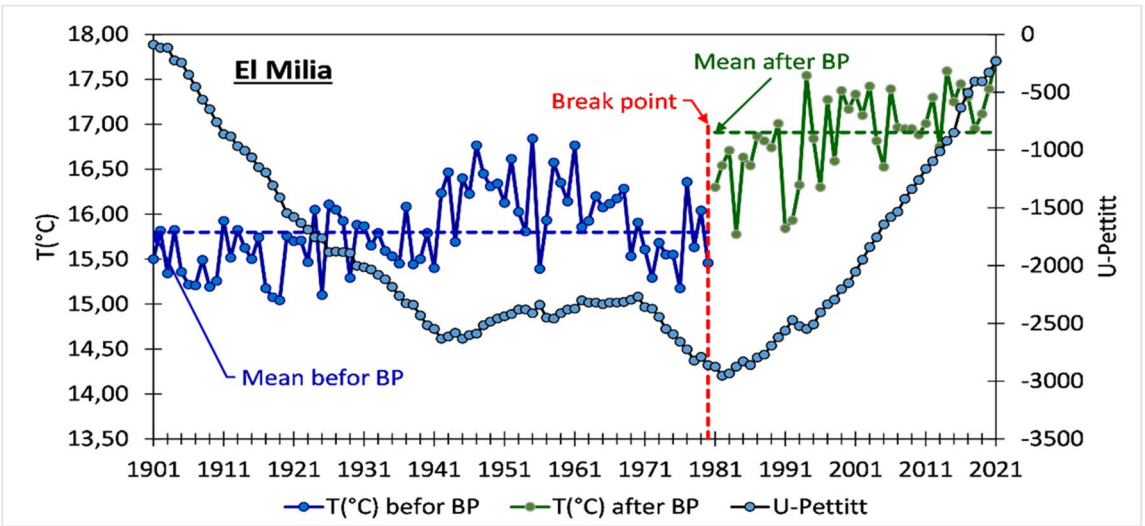
El Milia
Break point
Mean after BP
Mean befor BP
T(°C)
U-Pettitt
T(°C) befor BP
T(°C) after BP
U-Pettitt

◂**Fig. 2** Graphical representation of the temporal variation in mean inter annual temperature, the mean before and after the break in the series, and the Pettitt U variable

2.3 Methodology

After site selection, inventory, station selection and temperature data collection, statistical tests are applied to time series of mean temperature values, to highlight climate change within a period from 1901 to 2021. The main tests used are Hubert's segmentation procedure, Sen's slope, Pettitt's test, Mann–Kendall's test, and Buishand's test (Fig. 3).

The use of the free software "Khronostat" (http://www.hydrosciences.org/index.php/2020/09/04/khronostat/) enabled these tests to be applied to the time series (temperatures) of the Kebir Rhumel watershed. This watershed is covered by around forty climate stations, spread over seven sub-watersheds (Fig. 1), of which we have selected seven geographically representative stations (Table 1), which are Chebabta, Tiberguent, Tadjnanet, Ain Smara, Guerrah, Grarem Gouga, and El Milia. The temperature series used are composed of 121 years of average monthly and annual data calculated from daily values. The homogeneity test was performed with XLSTAT (free version).

2.4 Homogeneity

Statistical analysis of meteorological data time series is one of the tools used to identify trends in climatic variations. This analysis usually involves applying and interpreting statistical tests based on the homogeneity of the series (Lubes-Niel et al. 1998; Beaulieu 2009). The tests used in this work are described briefly.

2.5 Mann–Kendall

Statistical analysis of time series of hydro meteorological data is one of the tools used to identify climatic variations. This analysis most often involves the implementation and interpretation of statistical tests for series homogeneity (Beaulieu 2009; Lubes-Niel et al. 1998). The tests used are described briefly below.

2.5.1 Mann–Kendall

The most frequently used non-parametric test for identifying trends in hydrological variables is the Mann–Kendall (MK) test (Yadav et al. 2014). In this approach, the differences between each sequential value are calculated to represent increasing (+1), decreasing (−1) and neutral (0) signs, sgn (…), which is defined as Eq. (1) (Güçlü 2018; Yadav et al. 2014):

$$S = \sum_{k=1}^{n-1} \sum_{j=k+1}^{n} sgn(x_j - x_k) \tag{1}$$

It is clear that depending on the value of S, a monotonic trend is identified in the time series, as $S<0$ ($S>0$) decreasing (increasing). The other statistical parameter for the MK trend test is the standard Z value, given as follows:

$$Z = \begin{cases} {}^{S-1}\Big/_{\sqrt{V(S)}} \; for\; S > 0 \\ 0 \; for\; S = 0 \\ {}^{S+1}\Big/_{\sqrt{V(S)}} \; for\; S < 0 \end{cases} \tag{2}$$

In this expression, V(S) is the variance and in the case of equal ranks, where m is the number of linked groups, and *ti* is the number of observations in the *i*th group, it is given as Eq. (3):

$$V(S) = \frac{n(n-1)(2n+5) - \sum_{i=1}^{m} t_i\left(t_i - 1\right)\left(2t_i + 5\right)}{18} \tag{3}$$

The trend is considered insignificant if Z is below the confidence levels ($\alpha = 5\%$), but significant if $Z \geq Z\alpha/2 = \left| \pm 1.96 \right|$. On the other hand, the hypothesis (H_0) for significant trend, rejection is valid while acceptance is considered for the case of no trend (Ahmad et al. 2015; Baig et al. 2021; Braud 2011; Elmeddahi et al. 2016; Smadi and Zghoul 2006; Xavier Júnior et al. 2020).

2.6 Pettitt test

The Pettitt test (Smadi and Zghoul 2006; Braud 2011; Azzi and Chihati 2017; Ble et al. 2021) consists of decomposing the main series of N elements into two sub-series of size m and n, at each time t between 1 and N-1. The main series shows a break at time t if the two sub-series have different distributions. The absence of a break in the series of size n constitutes the null hypothesis. If the H_0 null hypothesis is rejected, an estimate of the date of the break is given at this time, defining the maximum absolute value of the variable U. The Pettitt variables (U) are defined by the following Eq. (4):

$$U = \sum_{\substack{0 \leq i \leq m \\ 0 < j < n}} D(i,j) \tag{4}$$

where D(i,j) = s g n (xi—xj).

s g n (x) = 1 if x > 0.

s g n (x) = 0 if x = 0.

s g n (x) = -1 if x < 0.

The probability (Prob) that a k value will be exceeded is defined and enables the significance of the break to be assessed (Eq. (5)).

$$\text{Prob (kn > k)} \approx 2 \;\; \exp / \text{Prob (kn > k)} \approx 2 \;\; \exp\left(-6k^2/n^3 + n^2\right) \tag{5}$$

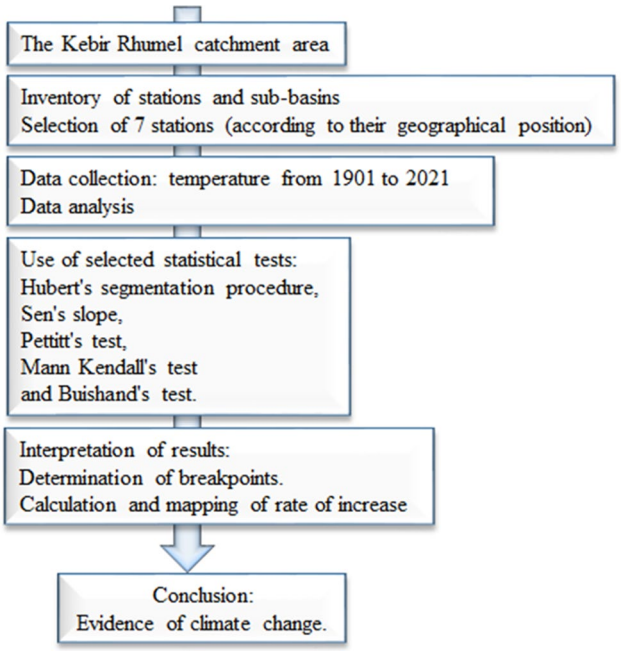

Fig. 3 Methodology flowchart

2.7 Sen's slope

Always considered as a complement to the MK test, or for both, the null hypothesis *H0* (absence of trend) is rejected when the level of significance or the eigenvalue (*p* value) is greater than 5%. When H0 is accepted, the slope of the trend (called Sen's slope) is estimated using Sen's method, where the slope is the median of all the slopes calculated between each pair of points. The robustness of the test has been validated by several comparison tests (Güçlü 2018; Drouiche et al. 2019).

2.8 Hubert segmentation

This method has the advantage of being able to search for multiple changes in the mean of a hydrometeorological series and can be used to deduce the break date. The principle is to divide the series into m segments ($m > 1$) so that the average of the neighboring segment(s) is significant, m being the rank of the initial series at the end of the Kth segment with $i_0 = 0 < i_1 < \ldots < i_k < \ldots < i_m - 1 < i_m < n$. The segmentation selected at the end of the procedure must be such that for a given segmentation order m, the squared deviation (Dm) is a minimum and the means of two contiguous segments are significantly different. This last constraint is satisfied by applying the Scheffé test (significance level of the Scheffé test: 1%), which is based on the concept of contrast (Kouassi et al. 2010; Azzi and Chihati 2017).

3 Results and discussion

Statistical methods are frequently applied to time series data to identify anomalies, which are interpreted as climatic changes, or more commonly calls: series break. Using this approach, on the series of temperature data (1901–2021) from the seven stations selected in the Kébir Rhumel watershed, we obtained the results presented in Table 2 and the graphs in Figs. 3, 4, and 5.

The graphs in Fig. 2 show the variation in the inter-annual mean temperature of the selected stations, where the Tadjenant station recording the lowest values with a minimum of 13.52 °C and a maximum of 14.23 °C. While the El Milia and Grarem Gouga stations have the highest values, with a minimum of 15 °C and a maximum of 17.7 °C.

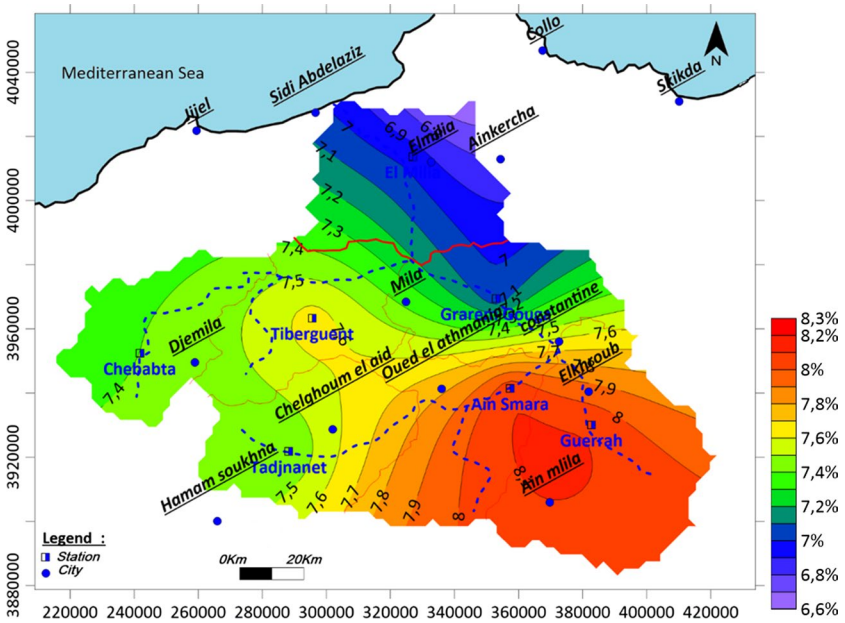

Fig. 4 Spatial distribution of the increase in mean inter annual temperature (in %), after the break point (1980) in the 1901–2021 series, in the Kébir Rhumel (WS 10)

We also note that for all seven stations, there is a breakpoint, which divides the series into two remarkable periods of consecutive years. The first from 1901 to 1980, with values below the average of the second period, that runs from 1981 to 2021. In general, the values are distributed around the average in a more or less alternating way between the minimum and maximum of each station individually.

Application of the Mann–Kendall test yielded values of Kendall's tau (Z) below the reference value, 1.96, with the interpretation that there is presence of an increasing trend, confirmed by the *S* value, which is greater than 0, for all the stations tested (Ahmad et al. 2015). The Sen's slope has values greater than 0 (positive) for all the stations tested, indicating an increasing trend (Ahmad et al. 2015). The Buishand test compares p to α, where $p < \alpha$, indicating a rejected H_0 (Güçlü 2018; Drouiche et al. 2019), which confirms the presence of a break year (point) for all tested stations.

Hubert's test was used to obtain the averages and standard deviations before and after the break point (BP), which enabled us to determine the rates of increase in temperature values at all the stations, as follows (Fig. 3): Chebabta 7.40%, Tiberguent 7.65%, Tadjenant 7.40%, Grarem Gouga 7.03%, El Milia 6.96%, Ain Smara 8.09%, and Guerrah 8.08%. The average for the whole watershed is 7.51%. The Scheffé test, with a value of 1%, is considered to be a validation condition for the Hubert test.

Calculating the averages of the series before and after the break point makes it possible to estimate the rate of increase, in percentage terms, of the mean annual temperature. This rate is spatially distributed on the map in Fig. 4 (kriging interpolation), where it can be seen to be increasing from north to south, from 7 to 8%. We also note that the lowest values are close to the sea, and the highest are located to the south of the Kebir Rumel watershed.

By calculating the rate of increase, it is possible to draw a map of the spatial distribution of the increase in inter annual mean temperature (in %), after the break point (1980) of the 1901–2021 series, in the Kébir Rhumel watershed (WS 10) (Fig. 2). This map shows that the rate of increase decreases from north (7%) to south (8%). It also varies, around 7% in the center of the watershed. The closer you get to the sea, the lower the rate of increase.

3.1 The L. Emberger climate index

Some authors (Daget 1977; Neira Mendez 2005) use the climatic index of L. Emberger, to update the climatic variability of a certain region; this index is calculated by the following formula:

$Q_2 = (P_i * 2000)/ (M^2—m^2)$, where P_i is the mean inter annual precipitation (in mm), M is the maximum monthly temperature of the warmest month in the series (in degrees Kelvin), m is the minimum monthly temperature of the coldest month in the series (in degrees Kelvin).

In our case, we calculated this index before and after the break point (BP), for the entire temperature series of the selected stations, and then represented it graphically

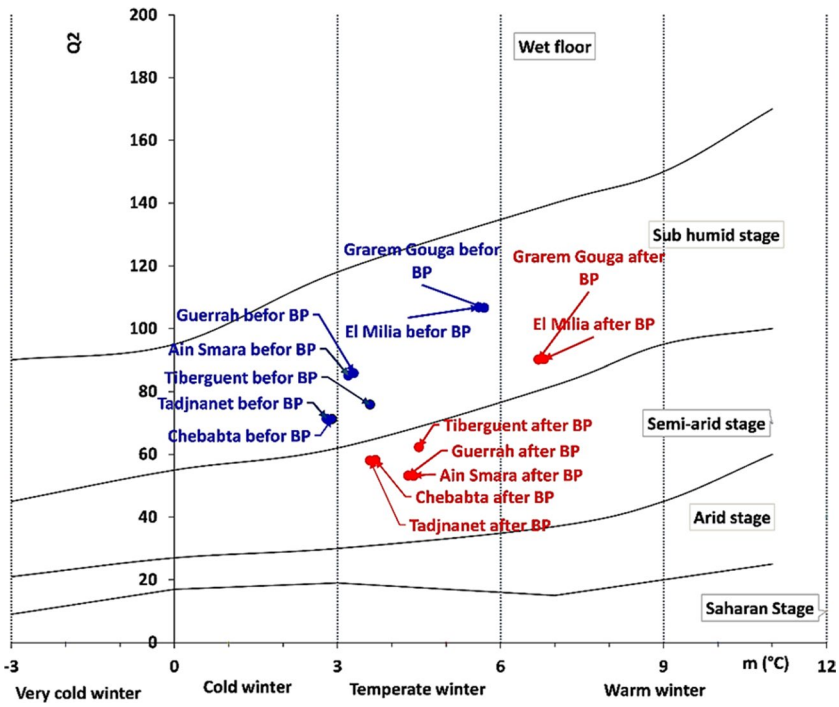

Fig. 5 Diagram of the L. Emberger climatic index, before and after the BP for the 1901–2021 series, for the stations selected on the Kébir Rhumel WS

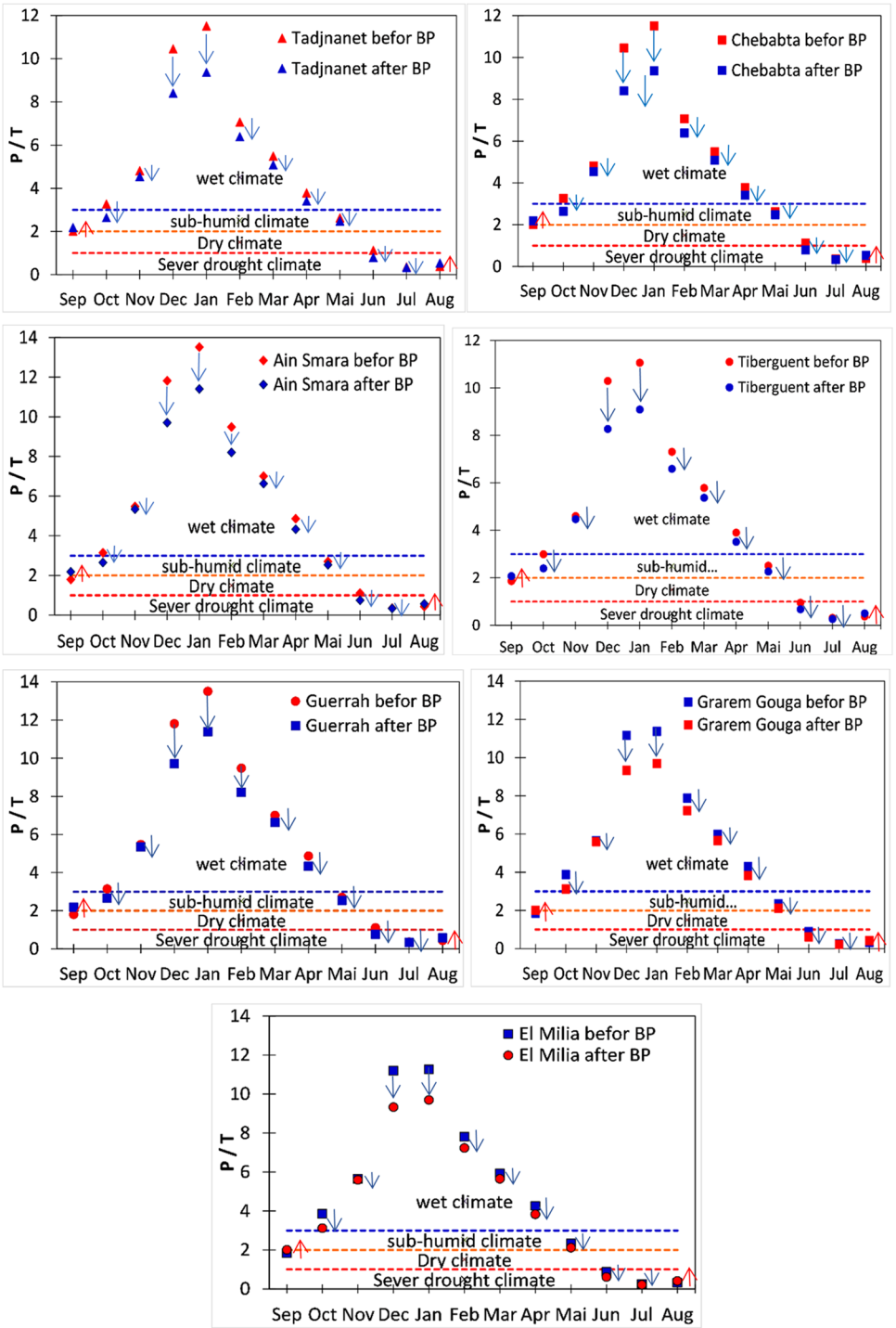

Fig. 6 Euverte method, before and after BP for the 1901–2021 series, in the Kébir Rhumel WS

(Fig. 5), where we note that the Tibergent, Ain Smara, Guerrah, Chebabta and Tadjnanet stations have moved from the sub-humid stage (before the BP) to the semi-arid stage (after the BP).

The Grarem Gouga and El Milia stations moved from the temperate winter (before the BP) to the warm winter (after the BP). These variations in the type of climate are mainly influenced by the increase in temperature.

3.2 Euverte method

This method is based on the P/T (precipitation/temperature) ratio, which is calculated from the monthly values of P and T, to define climatic regimes according to the result of the (P/T) ratio:

If $(P/T) < 1$, severe dry climate; with $1 < (P/T) < 2$, dry climate; with $2 < (P/T) < 3$, subhumid climate; and finally,

if (P/T) > 3, humid climate (Moral 1964; Euverte 1967; Kawalek 1980; Tefaha and Kihal 2016).

The application of Euverte's model to our series is shown graphically in Fig. 6, where 10/12 months have changed position, in the direction of a warmer climate (after BP).The months of November, December, January, February, March, and April show a trend from a humid climate (before BP) to a subhumid climate (after BP). September went from a dry climate (before the BP) to a sub-humid climate (after BP). The month of October went from wet climate (before BP) to severe drought climate (after BP). The month of June went from a dry climate (before BP) to one with severe drought climate (after BP). The month of July remained in the severe drought climate domain. The month of August shows a trend from severely drought climate (before BP) to dry climate (after BP).

4 Conclusion

This study analyzes the series of average monthly and annual temperature values for the period from 1901 to 2021 at 42 stations spread over the seven sub-watershed of the Kebir Rhumel, from which seven stations have been selected for their geographical location, making them representative of the watershed. Various statistical tests were applied to characterize climatic variability and highlight anomalies, in the time series, tested and interpreted in the climate change context. The Mann–Kendall (MK) test ($Z < 1.96$, $S > 0$) and the Pettitt test identified a break year, 1980, for all the stations in the Kébir Rhumel WS. The rate of temperature increase ranged from 6.96% at the El Milia station to 8.09% at Ain Smara. This rate is distributed spatially along a slight North–South slope. According to L. Emberger's climatic index, which expresses climatic variation before and after the break year, the position of 5/7 of the stations shifted from the sub-humid to the semi-arid zone. Finally, using the graphical representation of the Euverte model, we can see the trend in monthly values towards a warmer and less humid climate.

Acknowledgements We thank the anonymous reviewer for their constructive and valuable comments.

Author contribution All authors contributed to the conception and design of the study, the preparation, collection and analysis of the data, and the interpretation of the results. They have read and approved the manuscript.

Data availability The datasets generated and/or analyzed in this study are available from the corresponding author.

Declarations

Consent for publication The authors have read and approved the published version of the manuscript.

Competing interests The authors declare no competing interests.

References

Abdeddaim H (2018) Contribution à l'étude de l'influence de la structure du réseau hydrographique sur le risque hydrologique «Cas des bassins de l'Est de l'Algérie». Universite Mohamed Khider Biskra, Algeria, p 276

Ahmad I, Tang D, Wang T, Wang M, Wagan B (2015) Precipitation trends over time using Mann-Kendall and spearman's rho tests in swat river basin, Pakistan. J Adv Meteorol 2015:1–15. https://doi.org/10.1155/2015/431860

Ahmed K, Shahid S, Nawaz N (2018) Impacts of climate variability and change on seasonal drought characteristics of Pakistan. Atmos Res 214:364–374. https://doi.org/10.1016/J.ATMOSRES.2018.08.020

Aidat A (2017) Typologie de rapports entre la ville de Constantine et son Rhumel Boumerzoug. departement architecture et urbanisme. Magistere, Universite Mentouri –Constantine, Algeria, p 180

Akinsanola AA, Ogunjobi KO (2014) Analysis of rainfall and temperature variability over Nigeria. Global J Human-Soc Sci: B Geogr, Geo-Sci, Environ Disaster Manag 14:1–17

Asfaw A, Simane B, Hassen A, Bantider A (2018) Variability and time series trend analysis of rainfall and temperature in northcentral Ethiopia: A case study in Woleka sub-basin. Weather Clim Extremes 19:29–41. https://doi.org/10.1016/j.wace.2017.12.002

Azzi N, Chihati A (2017) Analyse statistique hydrologique dans un contexte de la variabilité climatique dans le bassin d'isser. departement Hydraulique. Université de Bouira, Algeria, p 89

Baig MRI, Naikoo MW, Ansari AH, Ahmad S, Rahman A, Environment (2021) Spatio temporal analysis of precipitation pattern and trend using standardized precipitation index and Mann–Kendall test in coastal Andhra Pradesh. Modeling Earth Systems Environment 2021:1–20. https://doi.org/10.1007/s40808-021-01262-w

Beaulieu C (2009) Homogénéisation des séries de précipitations: identification des techniques les plus prometteuses et nouveaux développements. Université du Québec, Institut national de la recherche scientifique, Quebec, p 336

Ble LO, Koffi FK, Degny GS, Soro TD (2021) Variabilité climatique et ressources en eaux de la région des grands ponts (Sud de la Côte d'Ivoire). J Synth: Rev Sci Et De La Technol 27:49–60

Braud I (2011) Méthodologies d'analyse de tendances sur de longues séries hydrométéorologiques. Fiche Techn Othu N 23:25–30

Collins JM (2011) Temperature variability over Africa. J Clim 24:3649–3666

Daget P (1977) Le bioclimat méditerranéen: analyse des formes climatiques par le système d'Emberger. Vegetatio 34:87–103

Dai A (2011) Drought under global warming: a review. Wiley Interdisc Rev: Clim Chang 2:45–65. https://doi.org/10.1002/wcc.81

Derdous O, Tachi SE, Bouguerra H (2021) Spatial distribution and evaluation of aridity indices in Northern Algeria. Arid Land Res Manag 35:1–14. https://doi.org/10.1080/15324982.2020.1796841

Di Cecco GJ, Gouhier TC (2018) Increased spatial and temporal autocorrelation of temperature under climate change. Sci Rep 8:14850. https://doi.org/10.1038/S41598-018-33217-0

Drouiche A, Nezzal F, Djema M (2019) Variabilité interannuelle des précipitations dans la plaine de la Mitidja en Algérie du Nord. Rev Sci Eau 32:165–177. https://doi.org/10.7202/1065205ar

Elmeddahi Y, Mahmoudi H, Issaadi A, Goosen MF, Ragab R (2016) Evaluating the effects of climate change and variability on water resources: a case study of the Cheliff Basin in Algeria. Am J Eng Appl Sci 9:835–845. https://doi.org/10.3844/ajeassp.2016.835.845

Euverte G (1967) Les climats et l'agriculture, Que sais-je ? edn. Presses Universitaires de France, France

Gilman SE, Urban MC, Tewksbury J, Gilchrist GW, Holt RD (2010) A framework for community interactions under climate change.

Trends Ecol Evol 25:325–331. https://doi.org/10.1016/J.TREE.2010.03.002

Güçlü YS (2018) Multiple Şen-innovative trend analyses and partial Mann-Kendall test. J Hydrol 566:685–704. https://doi.org/10.1016/j.jhydrol.2018.09.034

Kawalek A (1980) les zones agro-ecologiques de la republique centre africaine. Methodologie, limites des zones. bultins de service des sols -0002. CFA- FAO, BANGUI, p 125

Kouassi AM, Kouamé KF, Koffi YB, Dje KB, Paturel JE, Oulare S (2010) Analyse de la variabilité climatique et de ses influences sur les régimes pluviométriques saisonniers en Afrique de l'Ouest: cas du bassin versant du N'zi (Bandama) en Côte d'Ivoire. Cybergeo: Eur J Geogr 1–32. https://doi.org/10.4000/cybergeo.23388

Lubes-Niel H, Masson J-M, Paturel J-E, Servat E (1998) Variabilité climatique et statistiques. Etude par simulation de la puissance et de la robustesse de quelques tests utilisés pour vérifier l'homogénéité de chroniques. Rev Sci Eau 11:383–408. https://doi.org/10.7202/705313ar

Moral P (1964) Essai sur les regions pluviometriques de l'afrique de l'ouest. Ann Geog 73:660–686

Neira Mendez F (2005) Assessment of climate indices in drylands of Colombia. Msc Thesis, Universiteit Gent Belgium, p 123

Oulhaci D (2016) Ruissellement inter-annuel en Algérie septentrionale (Relation entre. Universite Kasdi Merbah Ourgla Algerie, Ruissellement Pluie et Evaporation), p 207

Panda A, Sahu N (2019) Trend analysis of seasonal rainfall and temperature pattern in Kalahandi, Bolangir and Koraput districts of Odisha, India. Atmos Sci Lett 20:e932. https://doi.org/10.1002/asl.932

Rauf AU, Rafi MS, Ali I, Muhammad UW (2016) Temperature trend detection in Upper Indus Basin by using Mann-Kendall test. Adv Sci, Technol Eng Syst J 1:5–13

Sam TT, Khoi DN, Thao NTT, Nhi PTT, Quan NT, Hoan NX, Nguyen VT (2019) Impact of climate change on meteorological, hydrological and agricultural droughts in the Lower Mekong River Basin: a case study of the Srepok Basin, Vietnam. Water Environ J 33:547–559. https://doi.org/10.1111/WEJ.12424

Singh P, Kumar V, Thomas T, Arora M (2008) Basin-wide assessment of temperature trends in northwest and central India/Estimation par bassin versant de tendances de température au nord-ouest et au centre de l'Inde. Hydrol Sci J 53:421–433. https://doi.org/10.1623/hysj.53.2.421

Smadi MM, Zghoul A (2006) A sudden change in rainfall characteristics in Amman, Jordan during the mid 1950s. Am J Environ Sci 2:84–91. https://doi.org/10.3844/ajessp.2006.84.91

Tefaha S, Kihal K (2016) Contribution à l'étude des impacts du barrage de Béni Haroun sur le plan climatique et hydrologique de la région de Mila. Centre Universitaire Mila, Algerie, p 80

Wang X, Liang P, Li C, Wu F (2014) Analysis of regional temperature variation characteristics in the Lancang River Basin in southwestern China. Quatern Int 333:198–206. https://doi.org/10.1016/J.QUAINT.2013.09.002

Wang Z, Li J, Lai C, Zeng Z, Zhong R, Chen X, Zhou X, Wang M (2017) Does drought in China show a significant decreasing trend from 1961 to 2009? Sci Total Environ 579:314–324. https://doi.org/10.1016/J.SCITOTENV.2016.11.098

Wu F, Wang X, Cai Y, Yang Z, Li C (2012) Spatiotemporal analysis of temperature-variation patterns under climate change in the upper reach of Mekong River basin. Sci Total Environ 427:208–218. https://doi.org/10.1016/J.SCITOTENV.2012.03.081

Xavier Júnior SFA, Jale JdS, Stosic T, Santos CACd, Singh VP (2020) Precipitation trends analysis by Mann-Kendall test: a case study of Paraíba, Brazil. J Revista Brasileira de Meteorologia 35:187–196. https://doi.org/10.1590/0102-7786351013

Yadav R, Tripathi S, Pranuthi G, Dubey S (2014) Trend analysis by Mann-Kendall test for precipitation and temperature for thirteen districts of Uttarakhand. J Agrometeorol 16:164–171